

Chaos around the superposition of a black-hole and a thin disk

Alberto Saa*

*Departamento de Matemática Aplicada,
IMECC-UNICAMP, C.P. 6065,
13081-970 Campinas, SP, Brazil*

Roberto Venegeroles†

*Departamento de Física Matemática,
Universidade de São Paulo, C.P. 66318,
05315-970 São Paulo, SP, Brazil*

Abstract

Motivated by the strong astronomical evidences supporting that huge black-holes might inhabit the center of many active galaxies, we have studied the integrability of oblique orbits of test particles around the exact superposition of a black-hole and a thin disk. We have considered the relativistic and the Newtonian limits. Exhaustive numerical analyses were performed, and bounded zones of chaotic behavior were found for both limits. An intrinsic relativistic gravitational effect is detected: the chaoticity of trajectories that do not cross the disk.

04.20.Jb, 95.10.Fh, 05.45.+b

Typeset using REV_TE_X

*e-mail: asaa@ime.unicamp.br

†e-mail: rveneger@fma.if.usp.br

In recent years, strong observational evidences have supported that huge black-holes, with masses between $10^6 M_\odot$ and $10^{10} M_\odot$, might inhabit the center of many active galaxies [1]. These evidences have motivated many investigations on the black-hole–disk system. Some approximate [2] and numerical [3] results were obtained, and in [4] some exact axisymmetric solutions describing systems containing the superposition of non-rotating black-holes and static thin disks are presented and discussed. Such systems have no net angular momentum, and a possible explanation for their stability is that the disk particles move under the action of their own gravitational field in such a way that there are as many particles moving to one side as to the other [5]. This counterrotating interpretation has been frequently used to describe true rotational effects (see, for spherical systems, [6] and, for cylindrical systems, [7]).

Here, we consider the integrability of oblique orbits of test particles in the exact static black-hole–disk system. There are examples in the literature of chaotic motion involving black-holes: in the fixed two centers problem [8], in a black-hole surrounded by gravitational waves [9], and in several core–shell models with relevance to the description of galaxies (see [10] for a recent review). We mention also that geodesic motions in some static axisymmetric spacetimes were considered in [11], where chaotic behavior was detected for several solutions containing N-point Curzon-like singularities.

We are mainly interested in bounded motions close to the black-hole, so one assumes that the disk is infinite and has an associated homogeneous Newtonian density. We have also considered the Newtonian limit of the black-hole–disk system, *i.e.*, we have also studied the integrability of oblique orbits of test particles under the Newtonian gravitational potential corresponding to the superposition of a monopole and an infinite homogeneous disk. Bounded zones of chaotic behavior were found for both the relativistic system and for its Newtonian limit. We also notice that the chaotic regions in the relativistic cases are typically larger than in the corresponding Newtonian ones. This is a consequence of an intrinsic relativistic gravitational effect we found: the chaoticity of trajectories that do not cross the disk.

Let us start by the Newtonian limit of the black-hole–disk system. The equations of motion for test particles in this case are very simple. We use cylindrical coordinates (r, θ, z) with the monopole, with mass M , located in the origin. The disk corresponds to the plane $z = 0$. The gravitational potential in this case is given by

$$V(r, \theta, z) = -\frac{M}{\sqrt{r^2 + z^2}} + \alpha|z|, \quad (1)$$

where α is a positive parameter standing for the mass density of the disk. The angular momentum L in the z direction is conserved, and we can easily reduce the three-dimensional original problem to a two-dimensional one in the coordinates (r, z) and with the Hamiltonian given by

$$H = \frac{\dot{r}^2}{2} + \frac{\dot{z}^2}{2} - \frac{M}{\sqrt{r^2 + z^2}} + \frac{L^2}{2r^2} + \alpha z, \quad (2)$$

for $z > 0$. For $z < 0$, H is obtained by substituting $\alpha \rightarrow -\alpha$. The Hamiltonian (2) is smooth everywhere except on the plane $z = 0$. Moreover, the parts of the trajectories restricted to the region $z > 0$ (or $z < 0$) are integrable. The Hamilton-Jacobi equations for a two-dimensional system with the potential

$$V(r, z) = -\frac{M}{\sqrt{r^2 + z^2}} + \frac{L^2}{2r^2} + \alpha z \quad (3)$$

can be separated in parabolic coordinates [12], leading to the second constant of motion

$$C = R_z - \alpha \frac{r^2}{2} = \dot{r}(z\dot{r} - r\dot{z}) - \frac{\alpha}{2}r^2 + \frac{Mz}{\sqrt{r^2 + z^2}} + L^2 \frac{z}{r^2}, \quad (4)$$

where R_z is the z component of the Runge-Lenz vector

$$\vec{R} = \frac{M}{\sqrt{r^2 + z^2}}(r\hat{r} + z\hat{z}) + \vec{v} \times \vec{L}, \quad (5)$$

where \vec{L} stands for the total angular momentum. In this case, with the two constant of motions H and C , the equations for the trajectories of test particles can be reduced to quadratures in parabolic coordinates [12]. We can take advantage of these results to study the trajectories of the original system (2).

Suppose that a bounded trajectory ($H < 0$) starts somewhere in the region $z > 0$. The time evolution of the trajectory will be governed by the integrable potential (3) until the plane $z = 0$ is reached, say at $r = r_1$, $\dot{r} = \dot{r}_1$, and $\dot{z} = \dot{z}_1 < 0$. After crossing the disk, the trajectory will be also governed by a potential like (3), but now with a negative parameter α . The trajectory evolves until the plane $z = 0$ is reached again, at $r = r_2$, $\dot{r} = \dot{r}_2$, and $\dot{z} = \dot{z}_2 > 0$, when the signal of α must be changed again in order to get the correct time evolution, and so on. The relevant Poincaré's section in this case will be given by the intersections $\{(r_1, \dot{r}_1), (r_3, \dot{r}_3), \dots\}$. Since the motion in the regions $z > 0$ and $z < 0$ are integrable, any irregularity in the oblique trajectories shall be credited to the signal changes of α between the integrable regions. In particular, trajectories that do not cross the disk are integrable, in contrast to the relativistic case, as we will see latter.

The trajectories in the integrable regions can, in principle, be described by means of Jacobi elliptic functions. The expressions are considerably complicated, and we have abandoned the hope of constructing analytically the Poincaré's sections. Nevertheless, we could construct them very accurately by solving numerically the system in the integrable regions and matching the trajectories appropriately on the disk plane. In the Figures 1 and 2, we show typical Poincaré's sections across the plane $z = 0$. Fig. 1 presents a low-energy situation ($H = -0.4, L = M = 1, \alpha = 0.1$) where the integrability seems to be preserved in a large region, while Fig. 2 presents a section ($H = -0.15, L = M = 1, \alpha = 0.1$) revealing a widespread chaotic behavior. We could obtain thousands of intersections for each trajectory with a cumulative error, measured by the constant H , inferior to 10^{-12} .

A key point is that the Poincaré's sections showed in Fig. 1 and 2 are present for any finite values of M and α . In particular, we will have wide zones of chaotic motion, as presented in Fig. 2, for any finite values of M and α . This is a consequence of the invariance of the equations of motion under the transformations

$$\begin{aligned} r &\rightarrow \lambda r, & M &\rightarrow M, & z &\rightarrow \lambda z \\ \alpha &\rightarrow \lambda^{-2}\alpha, & t &\rightarrow \lambda^{3/2}t, & L &\rightarrow \sqrt{\lambda}L, \end{aligned} \tag{6}$$

$$H \rightarrow \lambda^{-1}H$$

and

$$\begin{aligned} r &\rightarrow \lambda' r, & M &\rightarrow \lambda' M, & z &\rightarrow \lambda' z, \\ \alpha &\rightarrow \lambda'^{-1} \alpha, & t &\rightarrow \lambda' t, & L &\rightarrow \lambda' L, \end{aligned} \quad (7)$$

$$H \rightarrow H$$

$\lambda > 0$ and $\lambda' > 0$. Poincaré's sections are invariant, up to constant rescalings, under such kind of transformation, and hence it is possible to choose suitable values for L and H in order to have, for instance, the Poincaré's section of Fig. 2 for any finite values of α and M .

Now, let us focus the relativistic static black-hole–disk system. We start with the Weyl metric [13] describing static axisymmetric spacetimes,

$$ds^2 = -e^{\nu(r,z)} dt^2 + e^{\omega(r,z) - \nu(r,z)} (dr^2 + dz^2) + r^2 e^{-\nu(r,z)} d\theta^2. \quad (8)$$

The metric describing the superposition of a black-hole with mass M and a thin disk with homogeneous associated Newtonian density α can be obtained from the metric of a black-hole immersed in a pseudo-uniform field, which is described by the potentials

$$\begin{aligned} \nu(r, z) &= \alpha z + \ln \frac{R_1 + R_2 - 2M}{R_1 + R_2 + 2M}, \\ \omega(r, z) &= -\frac{\alpha^2}{4} r^2 + \ln \frac{(R_1 + R_2 - 2M)(R_1 + R_2 + 2M)}{4R_1 R_2} + \alpha(R_2 - R_1), \end{aligned} \quad (9)$$

where $R_1 = \sqrt{(M - z)^2 + r^2}$ and $R_2 = \sqrt{(M + z)^2 + r^2}$. The first terms in the right-handed side of (9) correspond to the pseudo-uniform gravitational potentials, which can be obtained from the Curzon metric by a limiting process [14]. They are called pseudo-uniform because their Newtonian limit corresponds to a uniform gravitational field. The potentials (9) satisfy Einstein vacuum equations everywhere except at the origin $r = z = 0$.

One can transform our metric in Weyl coordinates (t, r, θ, z) into spherical ones $(t, r_S, \theta, \varphi)$ by doing

$$r = \sqrt{r_S^2 - 2Mr_S} \sin \varphi, \quad z = (r_S - M) \cos \varphi. \quad (10)$$

For $\alpha = 0$, this coordinate transformation puts the line element (8), with the potentials (9), into the Schwarzschild form. From (10), one sees directly that the Schwarzschild radius $r_S = 2M$ corresponds in Weyl coordinates to the rod $r = 0$, $-M \leq z \leq M$, and that the circular equatorial photonic orbit at $r_S = 3M$, $\varphi = \pi/2$, corresponds to the orbit at $r = \sqrt{3M}$, $z = 0$. We note also that under the transformation (10), any infinitesimally thin disk in Weyl coordinates remains infinitesimally thin in spherical coordinates. For more details on the geometry of the Weyl metric, see [13] and the references therein.

Our black-hole-disk system corresponds to the juxtaposition of two black-hole-pseudo-uniform field solutions: the solution (9) for $z > 0$ and a solution with a reversed uniform field ($\alpha \rightarrow -\alpha$) for $z < 0$. The obtained metric has C^0 components and obeys Einstein vacuum equations everywhere except in the plane $z = 0$. The only nonvanishing components of the energy-momentum tensor are

$$\begin{aligned}\epsilon &= -T_0^0 = \alpha \frac{e^{\nu(r,z)-\omega(r,z)}}{4\pi} \left(1 - \frac{M}{\sqrt{M^2 + r^2}}\right) \delta(z), \\ p_{\theta\theta} &= T_3^3 = \alpha \frac{e^{\nu(r,z)-\omega(r,z)}}{4\pi} \frac{M}{\sqrt{M^2 + r^2}} \delta(z).\end{aligned}\tag{11}$$

Our solution obeys the weak energy condition ($\epsilon > 0$) everywhere. The counterrotating velocity V of the particles of the disk is given by $V^2 = p_{\theta\theta}/\epsilon$ [4]. For a relativistically consistent solution, one usually demands that $V^2 \leq 1$. For the present case

$$V^2 = \frac{M}{\sqrt{M^2 + r^2} - M}.\tag{12}$$

We have $V^2 \leq 1$ for $r \geq \sqrt{3M}$. If we change from the original Weyl to Schwarzschild coordinates, we find that it corresponds to $r_S \geq 3M$. Hence, we conclude that our solution is indeed relativistically consistent, since it is a well-known result that there are no circular orbits inside the photonic orbit ($r_S = 3M$). We are obtaining the consistent result that the centrifugal-gravity balance inside the photonic radius can only be maintained for superluminal velocities [4].

Now, we need the geodesic equations for the black-hole-disk system. Since one always has two independent Killing vectors for static axisymmetric spacetimes, the geodesic equations

for the Weyl metric (8) can be cast as

$$\begin{aligned}\ddot{r} + f_1(r, z) (\dot{r}^2 - \dot{z}^2) + 2f_2(r, z) \dot{r}\dot{z} + g_1(r, z) &= 0, \\ \ddot{z} + f_2(r, z) (\dot{z}^2 - \dot{r}^2) + 2f_1(r, z) \dot{r}\dot{z} + g_2(r, z) &= 0,\end{aligned}\tag{13}$$

where the dots denote derivation with respect to s . For the potentials (9), we have:

$$\begin{aligned}f_1(r, z) &= r \left\{ \frac{1/R_1 + 1/R_2}{R_1 + R_2 + 2M} - \frac{1/R_1^2 + 1/R_2^2}{2} - \frac{\alpha}{2} \left(\frac{1}{R_1} - \frac{1}{R_2} \right) - \frac{\alpha^2}{4} \right\} \\ f_2(r, z) &= z \left\{ \frac{1/R_1 + 1/R_2}{R_1 + R_2 + 2M} - \frac{1/R_1^2 + 1/R_2^2}{2} - \frac{\alpha}{2} \left(\frac{1}{R_1} - \frac{1}{R_2} \right) \right\} \\ &\quad - M \left\{ \frac{1/R_1 - 1/R_2}{R_1 + R_2 + 2M} - \frac{1/R_1^2 - 1/R_2^2}{2} - \frac{\alpha}{2} \left(\frac{1}{R_1} + \frac{1}{R_2} \right) \right\} - \frac{\alpha}{2} \\ g_1(r, z) &= h_1(r, z) \left[h_2(r, z) \frac{8M(R_1 + R_2)r}{(R_1 + R_2 + 2M)^2} - \frac{4R_1R_2L^2}{r^3} \exp(2\alpha z) \frac{R_1 + R_2 - 2M}{(R_1 + R_2 + 2M)^3} \right] \\ g_2(r, z) &= h_1(r, z) h_2(r, z) \left[\frac{8M(R_1(z + M) + R_2(z - M))}{(R_1 + R_2 + 2M)^2} + 2\alpha R_1R_2 \frac{R_1 + R_2 - 2M}{R_1 + R_2 + 2M} \right]\end{aligned}\tag{14}$$

where

$$\begin{aligned}h_1(r, z) &= \exp \left(\frac{\alpha^2}{4} r^2 + \alpha(R_1 - R_2) \right) \\ h_2(r, z) &= \frac{E^2}{(R_1 + R_2 - 2M)^2} + \frac{L^2}{r^2} \frac{\exp(2\alpha z)}{(R_1 + R_2 + 2M)^2}\end{aligned}\tag{15}$$

The expressions (14) and (15) are valid for $z > 0$. For $z < 0$, f_1 , f_2 , g_1 , and g_2 are obtained by doing $\alpha \rightarrow -\alpha$. The constants $E = -e^{\nu(r,z)}\dot{t}$ and $L = r^2 e^{-\nu(r,z)}\dot{\theta}$ are, respectively, the constants of motion associated to the Killing vectors $\partial/\partial t$ (the energy) and $\partial/\partial \theta$ (the z -angular momentum). Besides of these two constants, the requirement of a timelike trajectory leads to a further one

$$g_{ab}x^a x^b = -1 = e^{\omega(r,z) - \nu(r,z)} (\dot{r}^2 + \dot{z}^2) + \frac{L^2}{r^2} e^{\nu(r,z)} - E^2 e^{-\nu(r,z)}\tag{16}$$

We stress here that the system (14)-(16) corresponds to the simplest case of superposition of black-holes and disks. For the superposition with a non-homogeneous or a finite-radius disk, the metric tensor is considerably involved [4], and even the task of writing down the geodesic equations for oblique orbits seems to be unrealistic.

We could solve (13) numerically by using the same scheme used in the Newtonian case. However, we point out a crucial difference: the parts of the trajectories contained in the region $z > 0$ (or $z < 0$), in contrast to the non-relativistic case, are themselves non integrable. In other words, the trajectories of test particles around a black-hole immersed in a pseudo-uniform gravitational field are non integrable. This case should be added to the list of known examples of systems presenting qualitatively distinct behavior in their relativistic and Newtonian limits [15], stressing the deep differences between both theories. This fact clearly indicates that the relativistic black-hole–disk system is more chaotic than its Newtonian limit, and we could indeed verify that the chaotic regions in the relativistic limit are typically larger than in the corresponding Newtonian one.

Figure 3 presents a Poincaré’s section revealing a widespread chaotic behavior for the trajectories around a black-hole immersed in a pseudo-uniform field ($E = 0.975$, $L = 3.8$, $M = 1$, and $\alpha = 5 \times 10^{-4}$). We could obtain thousands of intersections for each trajectory with a cumulative error, measured by the constant (16), inferior to 10^{-12} . Since the relativistic equations are invariant under only one type of rescaling, our conclusions concerning the universality of the Poincaré’s section presented in the Fig. 3 are more limited than in the Newtonian case. It is not a surprise to find a strong chaotic behavior of the oblique orbits around the black-hole–disk system, since they are obtained by matching properly on the disk plane the (chaotic) trajectories of two black-hole–pseudo-uniform field systems.

We finish discussing our implicit assumption that there is no interaction between the test particle and the disk. It was assumed that the test particle may cross the disk many times without suffering any trajectory deviation. This can be an acceptable hypothesis if one considers the disk particles as very small when compared to the test particle and that we do not have many crosses. However, even in the case of very small disk particles, some trajectory deviation is expected to occur after a huge number of intersections. We have considered the following case of a weak interaction between the disk and the test particle: each time the test particle crossed the disk, its velocities (\dot{r}, \dot{z}) and L were perturbed by small and random amounts such that H (or E in the relativistic case) was maintained constant. Qualitative

equivalent Poincaré's sections were obtained. However, a more realistic interaction should also permit small changes in H (or in E). In other words, it would be worth to study the behavior of our models under more general stochastic perturbations [16]. These points are now under investigation.

ACKNOWLEDGMENTS

The authors are grateful to CNPq, DAAD, and FAPESP for the financial support. A.S. wishes to thank Prof. H. Kleinert and Dr. A. Pelster for the warm hospitality at the Freie Universität Berlin, where this work was initiated, and Prof. P.S. Letelier for stimulating discussions.

FIGURES

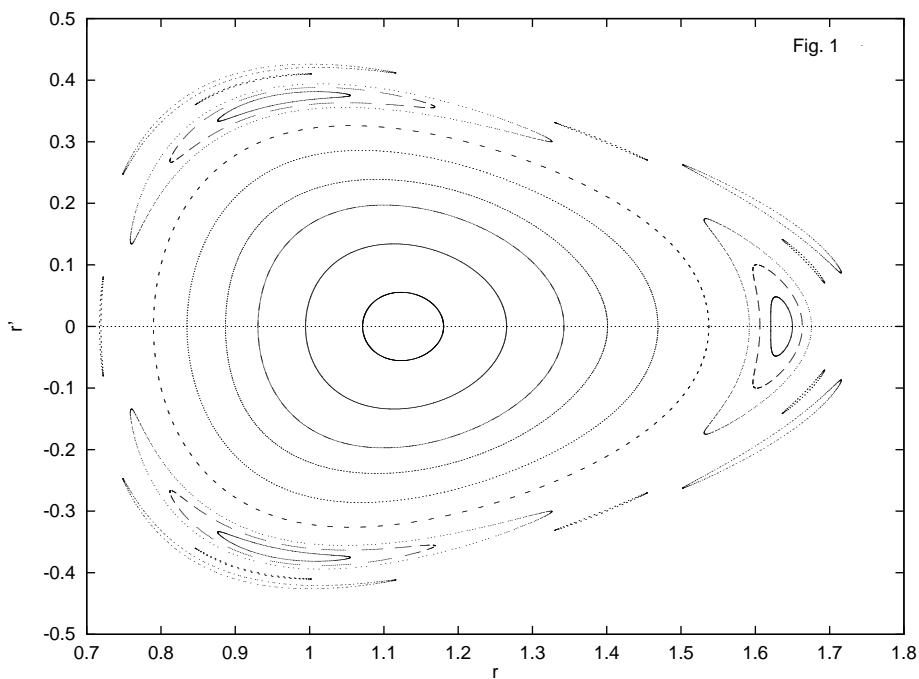


FIG. 1. Poincaré's section (r, \dot{r}) across the plane $z = 0$ for oblique orbits, with $H = -0.4$ and $L = 1$, around the superposition of a monopole with mass $M = 1$ and an infinity homogeneous disk with surface density $\alpha = 0.1$.

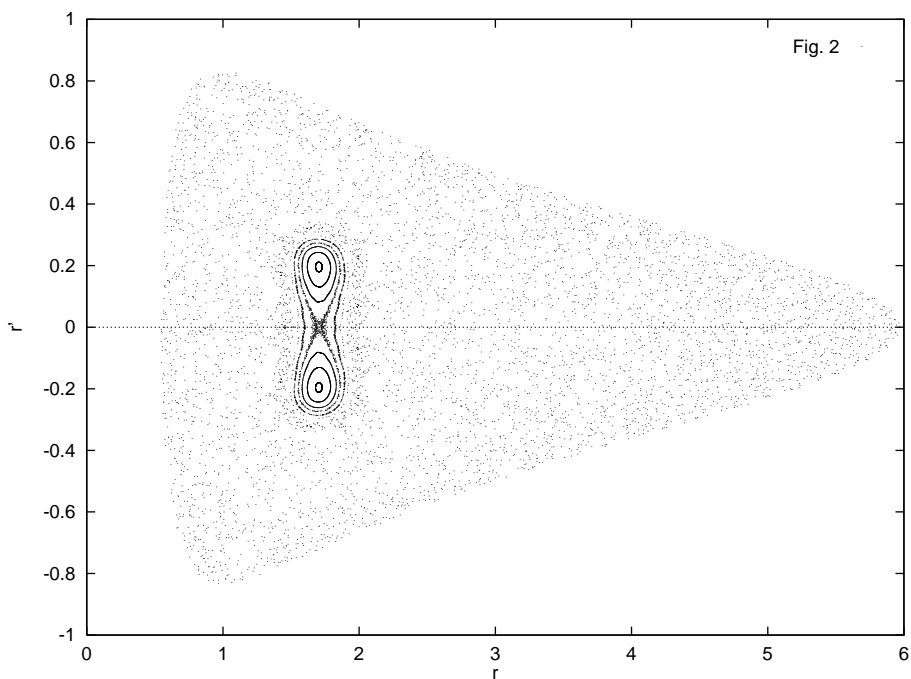


FIG. 2. Poincaré's section (r, \dot{r}) across the plane $z = 0$ for oblique orbits, with $H = -0.15$ and $L = 1$, around the superposition of a monopole with mass $M = 1$ and an infinity homogeneous disk with surface density $\alpha = 0.1$.

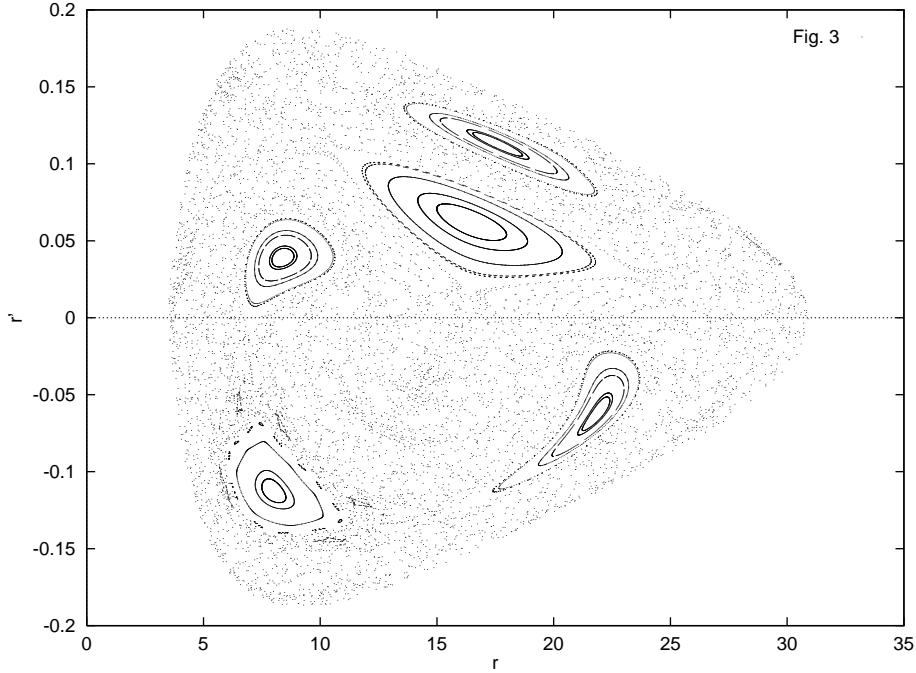


FIG. 3. Poincaré's section (r, \dot{r}) across the plane $z = 0$ for orbits with $E = 0.975$ and $L = 3.8$ around the exact superposition of a black-hole with mass $M = 1$ and a weak pseudo-uniform gravitational field ($\alpha = 5 \times 10^{-4}$).

REFERENCES

- [1] J. Kormendy and D. Richstone, *Astrophys. J.* **393**, 559 (1992). See also D. Lynden-Bell, *Nature* **223**, 690 (1969).
- [2] M.C. Begelman, R.D. Blandford, and M.J. Rees, *Rev. Mod. Phys.* **56**, 255 (1984).
- [3] A. Lanza, *Astrophys. J.* **389**, 141 (1992); S. Nishida, Y. Eriguchi, and A. Lanza, in *13th Conference of General Relativity and Gravitation*, edited by P.W. Lamberti and O.E. Ortiz (Universidad Nacional de Córdoba, Argentina, 1992).
- [4] J.P.S. Lemos and P.S. Letelier, *Phys. Rev.* **D49**, 5135 (1994).
- [5] T. Morgan and L. Morgan, *Phys. Rev.* **183**, 1097 (1969); **188**, 2544 (1969); **D2**, 2756 (1970).
- [6] A. Einstein, *Ann. Math.* **40**, 924 (1939).
- [7] T.A. Apostolatos and K.S. Thorne, *Phys. Rev.* **D46**, 2435 (1992).
- [8] G. Contopoulos, *Proc. R. Soc. Lond.* **A431**, 183 (1990); **A435**, 551 (1991); N.J. Cornish and G.W. Gibbons *Class. Quantum Grav.* **14**, 1865 (1997).
- [9] L. Bombelli and E. Calzetta, *Class. Quantum Grav.* **9**, 2573 (1992); P.S. Letelier and W.M. Vieira, *Class. Quantum Grav.* **14**, 1249 (1997).
- [10] W.M. Vieira and P. S. Letelier, *Astrophys. J.* **513**, 383 (1999).
- [11] Y. Sota, S. Suzuki, and K. Maeda, *Class. Quantum Grav.* **13**, 1241 (1996).
- [12] B. Dorizzi, B. Grammaticos, and A. Ramani, *J. Math. Phys.* **25**, 481 (1984); B. Grammaticos, B. Dorizzi, A. Ramani, and J. Hietarinta, *Phys. Lett.* **109A**, 81 (1985).
- [13] D. Kramer, H. Stephani, E. Herlt, and M. MacCallum, *Exact solutions of Einstein's field equations*, Cambridge University Press, 1979.
- [14] W.B. Bonnor, *Gen. Rel. Grav.* **20**, 607 (1988).

- [15] R. Moeckel, *Comm. Math. Phys.* **150**, 415 (1992); W.M. Vieira and P.S. Letelier, *Phys. Lett.* **228A**, 22 (1997).
- [16] Yu. Kifer, *Random perturbation of dynamical systems*, Birkhäuser, 1988; M. Viana, *Stochastic dynamics of deterministic systems*, unpublished lecture notes, IMPA, Rio de Janeiro, 1996.